# How fast is ultrafast chemistry?

**Biman Bagchi**

Solid State and Structural Chemistry Unit, Indian Institute of Science, Bangalore 560 012, India

**The field of ultrafast chemistry has seen a string of remarkable discoveries in the recent years. In this article we briefly discuss some of the problems solved recently. The understanding that has emerged from these studies has important consequences not only in chemistry but also in diverse biological processes.**

HOW fast is the response of a liquid to a given perturbation? The answer, of course, depends not only on the nature of the liquid but also on the nature of the perturbation itself. If the perturbation is slow, such as the shearing force on a liquid, then the response, the flow of the liquid, is also slow. And, if the perturbation is fast then the response is also fast. The question that a chemist has always asked is: How fast can this response be? What determines the limit? To a chemist, this question is not an idle one, but is profoundly related to the understanding of the effects of the solvent on the various chemical reactions[1–12] – we shall give examples later. And as the way we understand things now, the answer is also important to many biological reactions. Thus, we can formulate the question more precisely now: How fast is the response of chemically (and biologically) important solvents to various elementary chemical events that lead to much of the natural change around us?

The quest for the answer to the above question has occupied generations of chemists and finally the answer is beginning to take shape, thanks to some remarkable developments in this area in the last 3–5 years. For example, it was only very recently that the solvation dynamics of an ion in liquid water could be measured for the first time[11] – the dominant time constant is only about 50 fs (1 fs = $10^{-15}$ s)! No one had imagined that dynamics in water could be so fast. The importance of this particular experiment is that the dynamics was measured directly in the time domain. In fact, several such remarkable results have been obtained in the recent years. In the process many old ideas and notions have been found to be inadequate while new ones are still being tested. The objective of this article is to convey to the reader at least a part of the excitement of the field of ultrafast chemical dynamics.

There are many chemical reactions that occur at a great rate. It is only after the availability of ultrashort laser pulses and after the perfection of the associated detection techniques that study of these processes became possible. Figure 1 shows the evolution of time scales in the order they became available and a few examples of the dynamical processes which could be studied with the available time scales. It is important to realize that the underlying physical and chemical phenomena in different time scales are often profoundly different. In many cases the availability of shorter time scales meant more accurate measurement than was hitherto possible, often leading to new understanding. In some other cases completely new phenomena could be studied.

A key question in discussions on ultrafast processes is the limitation of the time scales posed by the Heisenberg uncertainty principle. When the time scales touch the femtosecond domain (the right bottom corner of Figure 1), then this certainly becomes a valid question. If we consider a relaxation that occurs with a time constant of 10 fs, then a quick calculation shows that the uncertainty principle imposes the limit that the minimum uncertainty in the frequency is $5 \times 10^{13}$ Hz or, equivalently, 125 $cm^{-1}$. Thus, the uncertainty principle may make studies of vibrational relaxation irrelevant in some cases. However, the chemical processes that involve electronic relaxation will not be affected. There are,

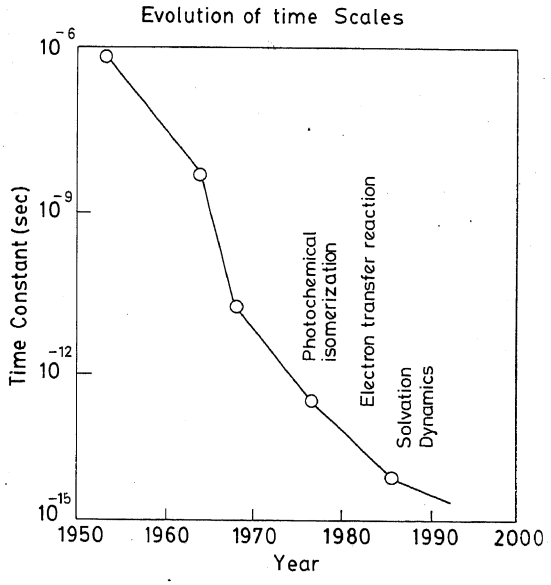


**Figure 1.** A schematic illustration of the evolution of time scales, where the experimentally accessible time constants of chemical processes are plotted against the years they became available. The three chemical relaxations discussed here, namely, isomerization dynamics, electron transfer reactions and solvation dynamics, are also shown in the same figure, approximately indicating the time when their modern studies became possible.

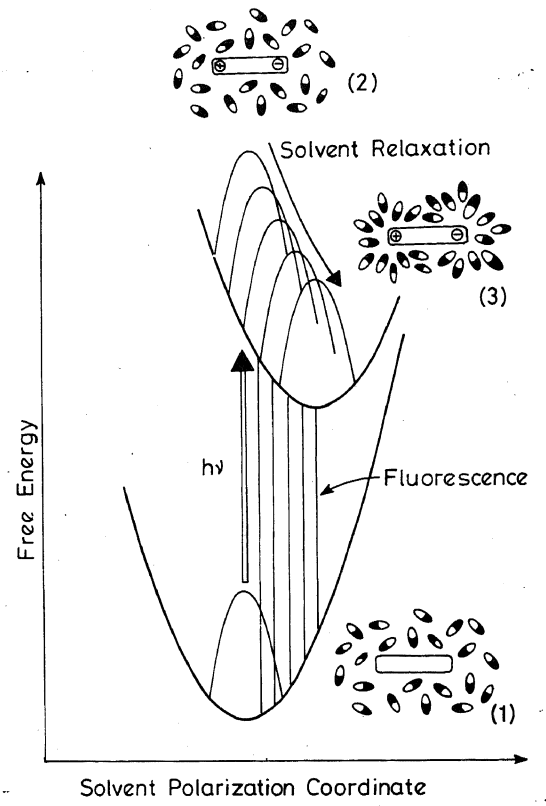


**Figure 2.** A schematic illustration of physical processes that accompany solvation dynamics and give rise to the time-dependent fluorescence Stokes shift (TDFSS). The state marked (1) is the unchanged, nonpolar state in equilibrium with the solvent. Optical excitation drives the system to the nonequilibrium state (2), where the solvent is still in the Franck–Condon state of the ground nonpolar molecule. Subsequent solvent reorganization leads to the stabilization (that is, solvation) of the polar molecule. As the system relaxes, the fluorescence from the solute shifts to the longer wavelength (that is, the spectrum gets red-shifted). The time dependence of this Stokes shift can be measured in experiments.

however, several other practical difficulties which make reliable study in the time scales below 20 fs difficult, at least at present. However, there may be interesting chemistry even in such short time scales. For example, the initial part of electron solvation dynamics after two-photon ionization of water molecules in liquid water occurs in times less than even 10 fs. During this time, the important process of the dephasing of the electronic wave function is virtually complete. It is not yet clear as to how to measure such processes.

In this review, we shall briefly touch upon a few of the chemical processes which have been studied intensely in the last few years. The examples are chosen from the author's own experience in the field, so they are not exhaustive. Also, the emphasis is entirely on the phenomena and their understanding – technical details (both experimental and theoretical) will be omitted. The list of references is not exhaustive. There are several reviews[1–8] and books[9, 10, 12] that have appeared in the last 5–6 years which contain the details and, in addition, provide useful starting point for the nonexpert. Boxes highlight the material expanding points briefly considered in the main text.

## Solvation dynamics in dipolar liquids

The study of solvation of chemical and biological molecules is as old as chemistry and biology. Very few people, therefore, expected solvation dynamics to occupy the centre stage in ultrafast chemical dynamics. However, things turned out differently for various reasons. First, polar dye molecules serve as excellent probes in the study of solvation dynamics as these molecules have large polar stabilization energy in the excited state. This is because these dye molecules, upon excitation, often undergo a large increase in the dipole moment, or sometimes may even photoionize. Therefore, optical excitation prepares the molecule in the Frank–Condon state, which is of much higher energy than the minimum of the potential energy in the excited-state surface. This situation is shown in Figure 2. Subsequent to excitation, the solvent molecules rearrange and reorient to stabilize the new charge distribution in the excited state. The resultant change in energy is the solvation energy, which, as already mentioned, may be several electron volts. The second reason for the choice of dye molecules as suitable probes is that they often have easily detectable fluorescence with long life times, so one can easily study the time dependence of the Stokes shift of this fluorescence as the solvation energy of the dye molecules evolves. This time dependence is described by the solvation time correlation function, which is defined as[13]

$$S(t) = \frac{E_{\text{solv}}(t) - E_{\text{solv}}(\infty)}{E_{\text{solv}}(0) - E_{\text{solv}}(\infty)}, \qquad (1)$$

where $E_{\text{solv}}(t)$ is the solvation energy of the newly created ion at time $t$. This function is defined such that it

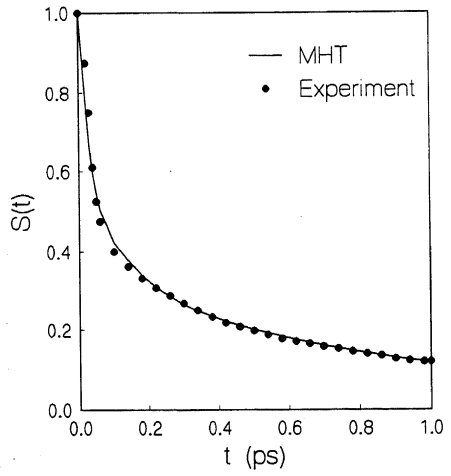


**Figure 3.** The solvation dynamics in liquid water. The black dots denote the experimental result[11], while the solid line is the theoretical prediction[24]. Note that the initial ultrafast part is over within 100 fs. For details, see the relevant references.

## Box 1.

In the experiment done by Jimnez *et al.*[11] a Coumarin 343 dye (sodium salt, $10^{-4}$ M), in water, is excited with an ultrashort optical pulse. The evolution of the fluorescence spectrum of the Coumarin 343 anion (Figure B1.1 *a*) has been studied to follow the solvation dynamics of the anion. The atom-centred charges in the ground state and in the excited state, after excitation by optical pulse, are shown below in Figures B1.1 *b* and *c*, respectively.

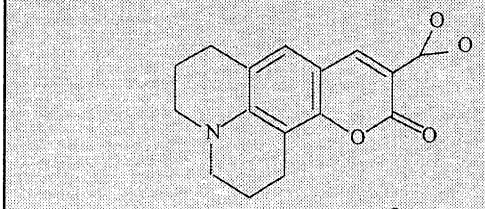


$C343^-$

(*a*)

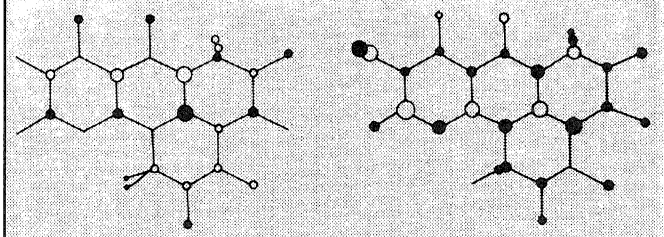

(*b*) (*c*)

The volume of each sphere is proportional to the charge on that atom and black denotes the negative charge. After excitation, the resultant fluorescence is resolved by a time-variable gate based on frequency-summing the fluorescence with a second ultrashort laser pulse (details given in the experimental section). As the solvent relaxation proceeds, there is a continuous shift of the emission spectrum towards the red end. The change in the peak frequency with time can be determined from these data. Thus, by observing the peak of the fluorescence spectrum at times $t$, zero and infinity, one can monitor the solvation dynamics of the anion and construct the solvation time correlation function $S(t)$ [vide equation (1)]. In the experiment a coherent Mira mode-locked Ti:sapphire laser has been used. The laser was operating at 850 nm. The second harmonic (425 nm), generated in a beta barium borate crystal, was used to excite Coumarin 343 (flowing in a quartz cell). The 850 nm light has been used to gate the fluorescence by mixing the fluorescence emission in another beta barium borate crystal. The cross-correlation of the two pulses (425 nm and 850 nm) was measured to be 100–110 fs (full width at half maximum). The intensity of the sum frequency has been measured as a function of the time delay between the two pulses. By angle-tuning the mixing crystal, emission decays were collected at certain intervals. The femtosecond fluorescence upconversion data obtained at a range of wavelenghts as a function of delay time has been plotted. These data can be used to construct a set of time-resolved emission spectra. The $S(t)$ can then be calculated from the set of spectra as discussed above.

decays from unity to zero as the solvation proceeds from $t = 0$ to $t = \infty$. The solvation dynamics is reflected in the red shift of the fluorescence spectrum and this experimental procedure is known as time-dependent fluorescence Stokes shift (TDFSS). One may expect that TDFSS will strongly depend on the nature of the solute probe, which can complicate the study of solvation dynamics. Fortunately, one finds that $S(t)$ is largely probe-independent, for reasons which are only partly understood, to be discussed later. The second reason for the great interest in solvation dynamics was the realization that it can significantly influence many chemical reactions, especially electron and proton transfers in polar liquids. Yet another reason is that the standard continuum model theories predicted that $S(t)$ would decay at a rate much faster than the rotational (and, of course, translational) relaxation. Thus, for water it predicted that the decay time would be about 250 fs (refs. 3, 13), which was startling even in the late eighties.

Over the last decade, $S(t)$ has been measured for a large number of polar molecules in different solvents. In the first phase (1986–1990), the experiments were done with time resolution only in the picosecond range. The solvation time correlation function was found to be non-exponential and differed from the predictions of the continuum models. During this period, an old comment of Onsager[14] became the topic of much discussion and we briefly discuss it here as it gave rise to interesting physics. In the Banff Conference on the 'Solvated Electron' in 1976, Onsager made the interesting comment that the polarization structure of an electron should form from outside in. That is, the molecules far from the electron should rearrange first, while the nearest-neighbour molecules relax the last. This suggestion came to be known as Onsager's 'inverse-snowball

## Box 2.

The theory of solvation dynamics has undergone rapid development in the last few years to keep pace with the experiments. The most successful of the theories assume a linear response of the dipolar liquid. Under this assumption, the non-equilibrium response function $S(t)$ (defined by equation (1) of the text) is equal to the equilibrium solvation-energy–energy time correlation function, $C_{EE}(t)$, defined by

$$C_{EE}(t) = \frac{\langle E_{solv}(0)\, E_{solv}(t)\rangle}{\langle E_{solv}(0)\, E_{solv}(0)\rangle}. \qquad \text{(B2.1)}$$

This assumption leads to the simplification that one needs to consider only an equilibrium time correlation function, which is simpler to deal with. The microscopic calculation of $C_{EE}(t)$ is somewhat involved and the details are beyond the scope of this review. However, if one assumes that the main component of the solvation energy of an ion is the interaction between the bare electric field of the ion and the dipolar molecules of the liquid, then the final expression is simple and is given by[22–25]

$$C_{EE}(t) = \frac{\int_0^\infty dk \left(\frac{\sin kr_c}{kr_c}\right)^2 \mathcal{L}^{-1}\left[1 - \frac{1}{\varepsilon(k, Z)}\right]}{\int_0^\infty dk \left(\frac{\sin kr_c}{kr_c}\right)^2 \left[1 - \frac{1}{\varepsilon(k)}\right]}, \qquad \text{(B2.2)}$$

where $\varepsilon(k, z)$ is the wavevector ($k$) and frequency ($z$) dependent dielectric function and $\varepsilon(k) = \varepsilon(k, z = 0)$ is the static dielectric function. $r_c$ is a cut-off distance due to the short-range nature of the repulsive interactions, $z$ is the (Laplace) frequency and $\mathcal{L}^{-1}$ denotes the Laplace inversion with respect to the frequency $z$. The standard dielectric constant is $\varepsilon_0 = \varepsilon(k = 0, z = 0)$. The above elegant expression has many satisfying features, one of them is that one recovers the well-known continuum model result simply by replacing $\varepsilon(k, z)$ by $\varepsilon(k = 0, z)$; the latter is the frequency-dependent dielectric function ($z$) measured in macroscopic experiments. The calculation of the wavevector- and frequency-dependent dielectric function forms the crux of the problem. This dielectric function $\varepsilon(k, z)$ can be shown to be given by the following expression[22]:

$$1 - \frac{1}{\varepsilon(k, z)} = \left(1 - \frac{1}{\varepsilon(k)}\right) \frac{1}{z + \Sigma(k, z)}, \qquad \text{(B2.3)}$$

where $\Sigma(k, z)$ is a generalized rate. This generalized rate derives contribution both from the rotational and the translational motions of the solvent molecules and also depends on the orientational pair correlation functions of the dipolar liquid. An important aspect of this rate is that in the absence of the translational contribution, it gives a smaller rate at intermediate wavevectors than at small values of $k$. This seems to agree with Onsager's 'inverse-snowball model' discussed in the text. However, when the translational component is efficient, then the complete reverse occurs, leading to the breakdown of the 'inverse-snowball model'. This theory has been applied to study solvation in many dipolar liquids. In Figure 3 the prediction of this theory has been compared with the experiments of Jimnez *et al.*[11] Note that the agreement is nearly perfect.

picture'. This also suggests that the solvation energy relaxation would be intrinsically nonexponential, as many, length-dependent, time scales are involved. Initial theoretical studies[15] supported this picture. However, it was argued later that the contribution of solvent translational modes may lead to the breakdown of the inverse-snowball picture[16]. More recently, it has been argued again that the Onsager picture may after all be correct for electron, but not for ions[17, 18]. The latest suggestion is that the electron being a very light particle will travel a long distance before it settles down in an existing trap. The dipolar molecules further from the electron can relax but the ones close to it must wait[18].

The most exciting experimental work on solvation dynamics has, however, taken place in the last 3 years only and the results will have far-reaching consequences. We shall refer to this period as the second phase. This started with the work on solvation of a dye, LDS-50, in acetonitrile reported from Fleming's laboratory at the University of Chicago[19]. This landmark experiment showed that solvation dynamics is biphasic with an ultrafast Gaussian component which decays with 80% of the total solvation energy within 200 fs. This is followed by a slow exponential-like decay with time constant of about 1 ps. This result was found to be in agreement with both computer simulation[20, 21] and theoretical[22] studies. However, the most interesting study, reported only last year, again from Fleming's group, is the solvation dynamics in water[11] (Box 1). As mentioned earlier, the results were remarkable. The solvation was found to be again biphasic. The initial Gaussian component decays with a time constant of less than 54 fs while the long time decay component can be described as a biexponential with time constants equal to 126 fs and 880 fs.

Figure 3 shows the solvation time correlation function in water. What is also interesting is the agreement of the long-time components with the earlier experimental results of Barbara and Jarzeba[3], who could not detect the ultrafast component because of limited time resolution. The solvation time correlation in methanol also contains an ultrafast Gaussian component with a time constant of about 70 fs. However, the relative weight of this part is somewhat less (about 30%) although still significant.

What is the origin of such ultrafast solvation in water, acetonitrile and methanol? These three liquids are quite different from each other and it is instructive to compare their dynamical features before we comment on the physical origin. Water, because of its small molecular weight and the extensive hydrogen bond network, has well-defined high-frequency vibrational modes. However, the single-particle orientation of water molecules is rather slow, with a correlation time of about 9 ps, due to the same hydrogen bonding. Acetonitrile, on the other hand, has fewer high-frequency vibrations, but orients very fast, with a correlation time of 0.3 ps. Methanol is again different. Because of chain-like hydrogen bond character, it has certain degree of high-frequency vibration, slow overall rotation but very fast rotation around the C–OH bond, which gives rise to a very fast polar response. All these details seem to be important in solvation dynamics[23].

We now turn to the explanation of the origin of the ultrafast component. Theoretical studies indicate[22–25] that all the natural fast dynamics of the system couple in different ways with the long-wavelength polarization fluctuation to give rise to the ultrafast component. This is because the main contribution to ion solvation energy comes from the long-wavelength part of the polarization, which is created in the liquid by the ion (Box 2). Now, the force constant for the longitudinal polarization fluctuation in a strongly polar dipolar liquid is large. Thus, the driving force to make ion solvation very fast exists in all strongly polar liquids. However, for solvation to be really fast, the liquid itself must be able to respond on the ultrafast time scale. This is where water and acetonitrile (and to smaller extent methanol and perhaps formamide) are exceptional. Water, due to its high-frequency vibrations and intermolecular vibrational modes, and acetonitrile, due to its fast rotational motion, can respond at a very high speed. The explanation given above is borne out by microscopic theory as shown in Figure 2.

Actually, even in these liquids, all is not ultrafast. Just as the rotation of water molecules is rather slow, so also the response to perturbations that vary on molecular length scales. These responses are also probed in many chemical processes, even in water. As discussed above, several rather unconnected (both microscopic and macroscopic) factors combine to give rise to the dominance of the ultrafast component in the solvation dynamics in water and acetonitrile.

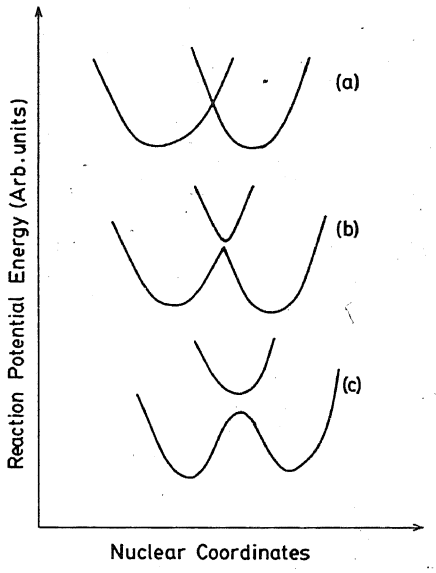


**Figure 4.** A schematic illustration of the nature of electron transfer reaction, based on the reaction potential energy surfaces. Depending on the strength of interaction between the two participating surfaces (corresponding to reactant and product states), the electron transfer can be classified as nonadiabatic, (case (a)), weakly adiabatic (case (b)) and adiabatic (case (c)).

## Electron transfer reactions

Electron transfer reactions are ubiquitous in chemistry and biology. The initial studies were motivated by the desire to understand acid–base equilibrium and also many organic reactions involving electron transfer as a key step. With the advent of laser it is now possible to study many kinds of electron transfer reactions, especially those occurring in the excited state, for the first time. The reason is that many of these reactions were found to proceed at exceedingly fast speed, often with time constants in the subpicosecond range. Well-known examples are electron transfer in a photosynthetic reaction centre, fluorescence quenching in excited betaines and ion pair formation in various charge transfer complexes. We address below only the recent advances in understanding solvent effects in ultrafast electron transfer reactions in solution.

The key to the great success of the Marcus theory[26] lies in the choice of the reaction coordinate. The motion of the system on the reaction potential energy surface along this coordinate takes the system from the reactant surface minimum to the product surface minimum. In conventional chemical picture, this coordinate is usually some distance or angle and its nature is clear from the beginning. The situation is different for the electron transfer reaction. In this case, often no chemical bond is broken or formed. The major part of the activation energy comes from the interaction between the reaction system and the dipolar liquid and not from any intra-

molecular potential. Thus, the reaction coordinate is collective in origin. In the Marcus theory the reaction coordinate is essentially the solvation energy difference between the reactant and the product. However, in order to specify the nature of any electron transfer reaction we must know the nature of interaction between the reactant and the product surfaces. Interestingly, this interaction itself is determined by the nature of the Born–Oppenheimer surfaces as a function of the nuclear coordinates. Thus, in order to understand the electron transfer reaction one must consider the potential energy surface as a function of both the reaction coordinate and the nuclear coordinate. The reaction potential energy surface for several cases is shown in Figure 4. If the reactant and the product surfaces interact very weakly, then the reaction can be considered as a transfer of the electron from the former to the latter at the crossing point and the reaction is termed 'nonadiabatic'. On the other hand, if the two surfaces interact strongly near the crossing, then the electron transfer occurs on one surface (which is given by a combination of the two parent surfaces according to the rules of quantum mechanics) and the reaction is termed 'adiabatic'. The experimental situation often lies between these two broad classifications and is termed loosely as 'weakly adiabatic' or even 'weakly nonadiabatic'. This intermediate situation is shown in Figure 4 *b*.

Recent studies[27–33] have critically examined the dynamic effects of solvent on various electron transfer reactions (Box 3). One is particularly interested to know what effects the newly discovered ultrafast solvation could have on electron transfer reactions. The answer depends on the 'adiabaticity' of the reaction. For nonadiabatic reactions even the ultrafast polar response was found to be not fast enough to affect electron transfer seriously. The situation is rather different for weakly adiabatic electron transfer. Here the first and foremost effect is that the rate of barrier crossing increases by almost an order of magnitude over the old estimates that ignored the ultrafast solvation effects[31–33]. This is true not only for water, but also for the other two ultrafast solvents, acetonitrile and methanol. For acetonitrile some additional interesting features appear. For this solvent the reactive friction (which arises from coupling between the electronic charge and the solvent) becomes so small that the electron transfer is controlled not by the rate of barrier crossing but by the rate of energy diffusion to the barrier from the reactant well. Electron transfers in water and methanol are predicted to be in the normal regime. In fact, it is rather ironic that ultrafast solvation in water implies that this solvent will be able to respond very fast to chemical changes during a reaction which, in turn, will not show any dynamic solvent effects[32, 33].

The Marcus theory predicts a parabolic dependence of reaction rate on the free energy of the electron transfer reaction (Box 4). Although this dependence was predicted in 1956, its verification had to wait till the 1984 landmark experiment of Miller *et al.*[34]. These authors measured the rate of electron transfer across a bridge of organic groups of varying length. Subsequently, several confirmations of the parabolic dependence have been reported[35]. However, there are also several recent studies of ultrafast electron transfer which found interesting breakdown of the Marcus parabolic dependence[36–40], due to various reasons. One such example is shown in Figure 5, where the rate of charge recombination (CR) of newly formed contact ion pair (CIP) is plotted against the free energy of reaction. The rate increases in the normal region with decrease in the free-energy gap. Murata and Tachiya[40] have recently provided an elegant explanation of this non-Marcus energy gap dependence by invoking the interplay between relaxation and electron transfer. A more detailed theoretical work by our group[41, 42] has shown that the above interplay can give rise to highly nonexponential decay of the reactant population.

## Box 3.

A very large number of experimental studies has been carried out in the recent years to understand various factors that influence electron transfer reactions. Three extensively studied examples are shown below:

(a) $Mn^{2+} + Mn^{3+} \Leftrightarrows Mn^{3+} + Mn^{2+}$

(b)

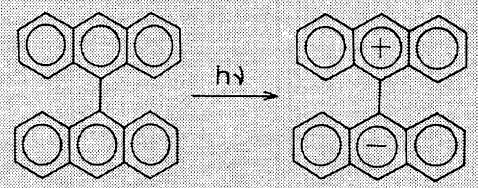

(c)

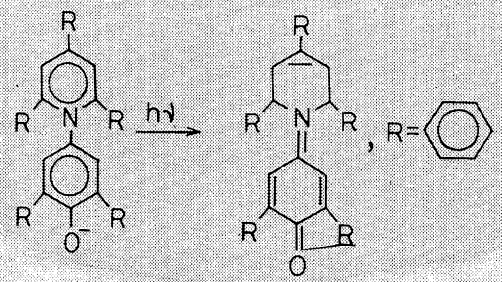

where (a), (b) and (c) correspond to the normal, zero-barrier and the inverted regime of electron transfer, respectively. Many different experimental techniques are being used routinely to study the dynamics of electron transfer. These include the rate of disappearance of fluorescence from the reactant well (due to electron transfer), femtosecond excited-state absorption and also the ground state recovery.

## Box 4.

In the Marcus theory, the reaction coordinate ($X$) is a collective quantity and is defined by the following expression:

$$X = \int d\mathbf{r}\, \Delta \mathbf{D}(\mathbf{r}) \cdot \mathbf{P}(\mathbf{r}), \qquad \text{(B4.1)}$$

where $\Delta \mathbf{D}(\mathbf{r})$ is the change in the displacement vector due to the charge redistribution owing to the electron transfer and $\mathbf{P}(\mathbf{r})$ is the polarization field. Note that here the reaction coordinate itself is an energy. The reaction potential energy has minima corresponding to the reactant and the product states. In the Marcus theory, electron transfer is considered to be mediated by solvent polarization fluctuations and distinction is made between the nonadiabatic and adiabatic electron transfers. For the former case, the rate is given by the following expressions:

$$k = (V^2/h)\,(4\pi\lambda / k_B T)^{1/2} \exp(-\beta E_a), \qquad \text{(B4.2)}$$

where $V$ is the nonadiabatic coupling between the two surfaces (determined by the nuclear coordinates). The activation energy $E_a$ has the following well-known form:

$$E_a = (\Delta G^0 + \lambda)^2 / 4\lambda, \qquad \text{(B4.3)}$$

where $\Delta G^0$ is the free energy gap and $\lambda$ is the solvent reorganization energy. In Figure B4.1 we show the potential energy surface to explain the notation.

In the adiabatic limit, the rate expression is different and is given by

$$k = \frac{\omega_R}{2\pi} \exp(-\beta E_a), \qquad \text{(B4.4)}$$

where $\omega_R$ is the harmonic frequency of the reactant well.

The above expressions are essentially transition state expressions. The important thing to note is the parabolic trend of the rate predicted by equation (B4.3) as a function of the free-energy gap $\Delta G^0$.

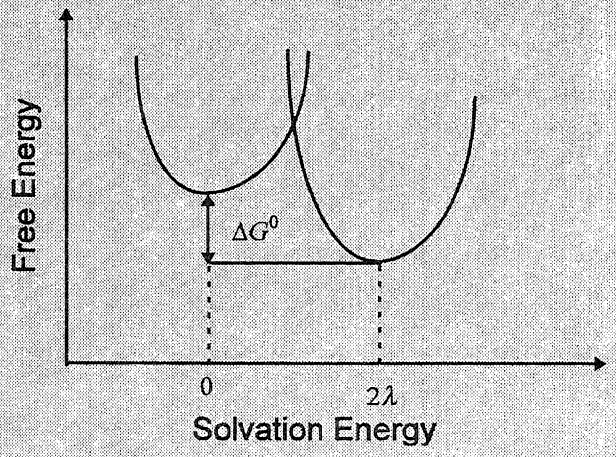


**Figure B4.1.** A schematic representation of the reaction free-energy surface, according to the Marcus theory. $\Delta G^0$ is the free-energy gap between the reactant and the product and $\lambda$ is the solvent reorganization energy. Note that the reaction coordinate (the abscissa) has been set to solvation energy.

Since the reaction coordinate is the fluctuating energy gap due to solvation, it is obvious that solvation dynamics will play an important role in determining the dynamics of electron transfer. Zusman was the first to quantify this dependence by deriving the following expression for an adiabatic reaction:

$$k = \frac{1}{\tau_L}(16\pi k_B T/\lambda)^{-1/2} \exp(-\beta E_a), \qquad \text{(B4.5)}$$

where $\tau_L$, the longitudinal relaxation time, is a measure of the solvation time of a newly created ion[1–10].

When the solvent polar response is ultrafast, like in water and acetonitrile, then the above expression for solvent effects undergoes significant modification. The theoretical work that accounts for ultrafast solvation is available in ref. 32. The main results are described in the text.

Another reason for the non-Marcus energy dependence is the involvement of high-frequency modes of the product state, which often serve as the accepting modes to accelerate electron transfer[37–39]. This mechanism is particularly useful when the electron transfer is in the Marcus inverted regime and results in the absence of the decrease of the rate as the free-energy change between the reactant and the product is made larger (that is, $G$ is negative and large). This mechanism of the non-Marcus energy gap dependence seems to be responsible for the large electron transfer rate observed recently in betaines[38].

## Isomerization dynamics

Isomerization reactions are very important chemical reactions. There are several reasons why these reactions often proceed at a very high speed. First, no chemical bond is broken or formed. The barrier is often rather small, only a few kcal/mol[43]. Moreover, there are several important reactions which proceed in the absence of any activation barrier. Some examples are the *cis* → *trans* isomerization of excited stilbene and also the isomerization of triphenyl methane dyes, such as malachite green[43]. These reactions are naturally very

## Box 5.

There are two classes of molecules which are particularly useful in the study of isomerization dynamics. These are stilbenes and the triphenyl methane dyes. The structures are shown below:

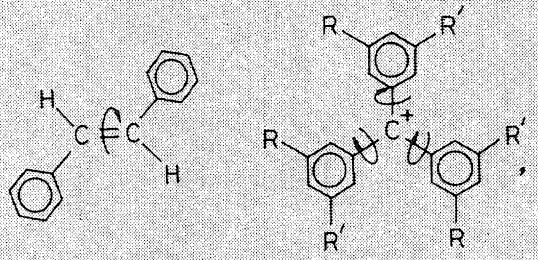


R, R′ = alkyl group

The reactive motion, in each case, is a twist of a group around a body-fixed axis, as shown by the arrows. The isomerization reaction is a high-barrier one for *trans* → *cis* isomerization in stilbene, but nearly barrierless for *cis* → *trans* for the same system. It is also barrierless in a large number of TPM dyes, like crystal violet and Malachite green.

Experimentally, these molecules are often studied by exciting them to a higher electronic state. The dynamics of isomerization is then studied by monitoring the decay of fluorescence from these dyes. Since isomerization leads to the formation of a new state, the fluorescence from the reactant gets quenched as the reaction proceeds. Thus, the time dependence of the decay of fluorescence intensity serves as an excellent probe of isomerization dynamics. The experiments have usually concentrated on the temperature and viscosity dependence – the latter often shows very interesting fractional viscosity dependence. However, the latter problem, despite considerable effort over the last two decades, has remained largely ill-understood. This is because the potential energy surfaces of isomerization reactions appear to be rather sensitive to their environment. For example, the activation energies change significantly when the solvent is changed. Even the change of temperature affects the activation energy because the properties of the solvent often change significantly with temperature. This is also true, perhaps to a lesser extent, for pressure change. Thus, one is left with very limited scope for changing the viscosity of the solvent without affecting the reaction potential energy surface. Thus, computer simulations appear to be the ideal method to bridge the gap between theory and experiments.

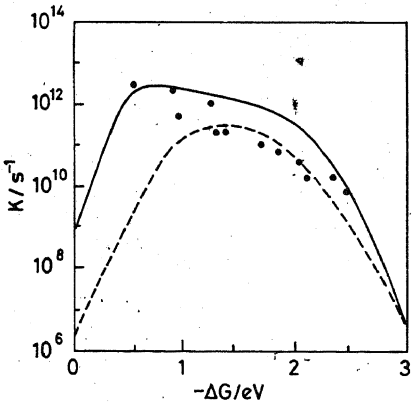


**Figure 5.** Breakdown of the Marcus parabolic dependence on the free-energy gap for charge recombination in newly formed contact ion pair. The black circles denote the experimental results of Asahi and Mataga[36] while the solid line is the theoretical prediction of Murata and Tachiya[40]. The Marcus parabola is also shown by the dashed line.

fast. There are some cases also where the barrier is significant. In other words, the isomerization reactions span a diverse range in kinetic behaviour. Because of the simplicity of these reactions, they serve as the testing grounds for the theoretical models of solvent effects. We shall discuss here two important and recent theoretical developments which were initially motivated by experimental results on ultrafast isomerization reactions in solution but led to far-reaching consequences (Box 5).

Before 1980, the effects of solvent viscosity on isomerization reaction were explained by using the well-known Kramers' theory[44]. This theory assumes that a chemical reaction can be viewed as the passage of a Brownian particle over an activation barrier. For large solvent viscosities, this theory predicts that the rate is inversely proportional to the viscosity. This is a straightforward consequence of modelling the reaction as a Brownian motion. Initial experiments seemed to have supported this. Detailed experimental studies could be undertaken only after picosecond laser became available in the early eighties. The new experimental results clearly indicated that for fast isomerization reactions (with lifetimes in the picosecond and even in the subpicosecond range) in solution, Kramers' theory was inadequate to explain the viscosity dependence – the observed viscosity dependence was much weaker than the inverse dependence predicted by Kramers' theory[45–47].

**Box 6.**

The recent experimental results from the study of isomerization dynamics have played a key role in the development of modern chemical reaction theory. Not only did these results motivate newer studies, but they also serve as the testing ground for the older theories. Here we discuss one particular class of theories which have been quite successful in explaining the viscosity dependence of the rates. Prior to 1980, the only theoretical framework available in this area was that due to Kramers, who modelled a chemical reaction as the motion of a solute in a one-dimensional double well potential. The reaction occurs when the solute escapes from one well to the other and in the process needs to go over the potential barrier, which is modelled as an inverted parabola of frequency $\omega_b$. Kramers assumed that the equation of motion was an ordinary Fokker–Planck equation. This second-order partial differential equation could be solved for the steady-state solution, which gives the following expression for the rate:

$$k = \frac{\omega_R}{2\pi\omega_b}\left[\left(\frac{\zeta^2}{4}+\omega_b^2\right)^{1/2}-\frac{\zeta}{2}\right]\exp(-\beta E_a), \quad \text{(B6.1)}$$

where $E_a$ is the activation energy, $\omega_R$ and $\omega_b$ are the harmonic frequencies of the reactant well and of the barrier top, respectively. $\zeta$ is the friction on the reactant motion. For isomerization reaction, this friction may be proportional to the viscosity of the solvent. Kramers' expression predicts that at high viscosities (that is, larger than 10 cP), the rate should be proportional to viscosity. However, experiments indicate that for many reactions with high barrier, the rates show a much weaker (such as, fractional) viscosity dependence. In 1980, Grote and Hynes[49] presented a generalization of Kramers' theory. These authors pointed out that Kramers' theory may be inadequate because it neglects the memory of motion along the reaction coordinate. The generalized rate is obtained by solving the following relation self-consistently:

$$\lambda_r = \frac{\omega_b^2}{\lambda_r + \hat{\zeta}(\lambda_r)}, \quad \text{(B6.2)}$$

where the factor $\lambda_r$ gives the required rate by $k = \lambda_r k^{TST}$, $k^{TST}$ being the transition state rate. In the above equation, $\hat{\zeta}(x)$ is the frequency-dependent friction, which gives the viscoelastic response of the solvent. As explained in the text, a reaction with a sharp barrier can probe only the high-frequency component of friction, which can be vastly different and much smaller than the zero-frequency friction that enters in Kramers' theory. This can explain the weak viscosity dependence of rate in many isomerization reactions. However, as described in Box 5, experimental difficulties have not yet allowed a full, convincing comparison between theoretical predictions and the experiments.

This started a flurry of theoretical activity[48–51]. Interestingly, the work that proved to be the most useful in this stage was published only a few years ago by Grote and Hynes[49]. The understanding that has emerged is the following. In *cis* ↔ *trans* isomerization reactions, the two potential energy minima are often separated by a dihedral angle lying between 90° and 180°. This gives rise to a sharp barrier when the activation energy barrier is somewhat larger than 10 kcal/mol. A sharp activation barrier implies that the reactant spends very little time in the barrier region and, therefore, probes only the high-frequency part of the solvent frictional response. The relation between the barrier height and the barrier curvature has been illustrated in Figure 6. This is to be contrasted with Kramers' theory, which assumes a slow diffusive motion along the reaction coordinate across the barrier (Box 6). For a sharp barrier only the former picture is valid. Since at large viscosities the high-frequency frictional response of the liquid gets decoupled from the macroscopic (that is, zero frequency) viscosity, the reaction rate also gets decoupled from viscosity and this shows up as a weak dependence of the reaction rate on the solvent viscosity. This rather elegant explanation is also known as the non-Markovian effect in barrier crossing.

Another class of isomerization reaction has drawn attention in the recent years[43, 52–54]. This is the zero-barrier reaction limit. As already mentioned, several important photochemical reactions fall in this limit. Consider that a molecule is optically excited and that in the excited state there is a photochemical funnel at the minimum of the excited-state surface. The motion that takes the system from its initial state to the final state is the reactive motion. The situation is depicted in Figure 7. This reactive motion can be the rotation of a bulky, molecular group (as in the case of TPM dyes). In this case the rate of reaction can be very high and dependent on the solvent viscosity. For *cis* → *trans* isomerization of stilbene in hexane, the isomerization rate seems to be as high as $10^{13}$ $s^{-1}$ (refs. 53, 54). This is one of the fastest rates

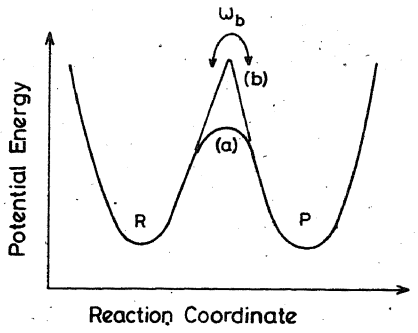


**Figure 6.** A schematic illustration of the dependence of the curvature of the activation barrier of the isomerization reaction on the barrier height. As the barrier height increases, the barrier frequency ($\omega_b$) also increases, leading to the decoupling of the rate from the solvent viscosity.

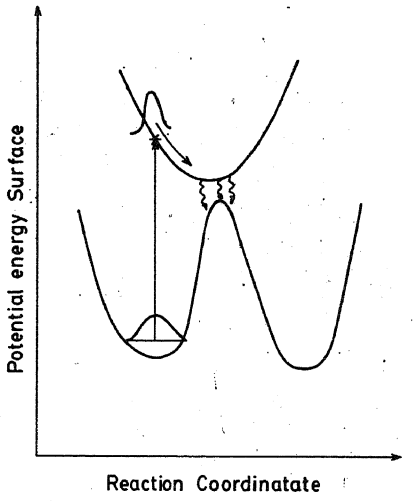


**Figure 7.** A schematic illustration of a zero-barrier chemical reaction. Initial excitation places the molecule in a nonequilibrium position on the excited-state potential energy surface. Subsequent relaxation brings the molecule to the potential minimum, where a photochemical funnel (or a sink) is present, This funnel gives rise to the decay of the excited state. The reactive motion is the relaxation from the initial excitation position to the configuration where the sink is located.

measured in the condensed phase. The decay of population on the excited state can often be measured by studying the disappearance of fluorescence from the excited state or by the recovery of the ground state population. An important characteristic of this type of reaction is that the time dependence of the excited-state population is highly nonexponential. Another important hallmark of barrierless reactions is the fractional viscosity dependence of the rate. The reason for the fractional viscosity dependence here is rather different from that in the high-barrier reaction and is often the multidimensional nature of the reaction potential energy surface; the second dimension may be a solvent mode or an intramolecular vibrational mode.

The theoretical studies of barrierless reactions are mostly based on a stochastic approach, where a Smolu-chowski or a Fokker–Planck equation is used to describe the motion on the reaction potential energy surface with a coordinate-dependent sink term to account for the decay from the photochemical funnel. This approach[43] seems to have been fairly successful in describing the experimental results.

## Ultrafast chemistry in biological processes

It should be pointed out that it is a fairly recent realization that the barrierless chemical reactions are quite common not only in chemistry but also in biological reactions. The most famous examples are the electron transfer in the reaction centre in photosynthesis[55] and the isomerization reaction in rhodpsin, which triggers the proton pump in the retinal membrane. These discoveries have led to very interesting chemistry. In what follows, we briefly discuss a very recent theoretical work by Chandler *et al.*[56] that led to valuable insight into the electron transfer mechanism in the photosynthetic reaction centre. A schematic representation of the relevant part of the reaction centre is shown in Figure 8. It is known that after the photoexcitation, the electron transfer takes place from 1 to 3 along the right-hand side of the figure. The theoretical work mentioned above has suggested that the reason for this selective transfer is that this reaction is barrierless while the $1 \rightarrow 2$ transfer involves a sizeable activation barrier[56]. A schematic drawing of this situation is shown in Figure 9. Another important example is the isomerization of bacteriorhodopsin in the retinal membrane, halobrium halobacterium. This is also a barrierless reaction with a time constant of 0.5 ps (refs. 57, 58). This reaction has recently raised a lot of interest. Yet another example of much current interest is the recombination of oxygen and carbon monoxide with the iron in heme in myoglobin[59, 60]. Flash photolysis studies have shown that this reaction follows a nonexponential kinetics. Interesting theoretical work has been done on this problem. Much experimental, computer simulation and theoretical studies have been done on the dynamics of proteins, which seem to have relaxation over a range of time scales. As the technique of ultrafast spectroscopy becomes more and more refined, we can look forward to many more fascinating applications of ultrafast chemistry to biological systems.

In the past many experts have raised the following question: What could be the relevance, if any at all, of the ultrafast chemistry to biology when the life processes occur on much slower time scales? This is certainly a valid question. With the recent discoveries of ultrafast biological processes (such as electron transfer in a photosynthetic reaction centre), this question needs to be reformulated as follows: Why does Nature use so

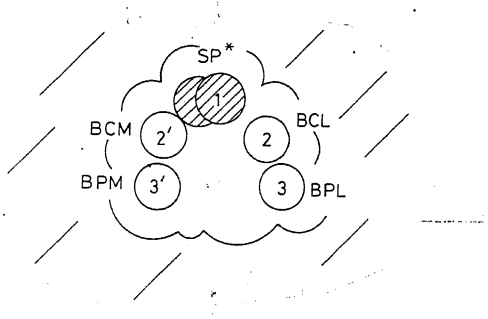


**Figure 8.** A schematic depiction of the essentials of the primary electron transfer event in a bacteria photosynthetic reaction centre. SP* denotes the photoexcited special pair. The electron, in principle, can be transferred either to the L branch, forming the charge-separated states $SP^+ BCL^-$ or $SP^+ BPL^-$, or it can go to the M branch, forming similar states. The experimentally observed case is $SP^+ BPL^-$.

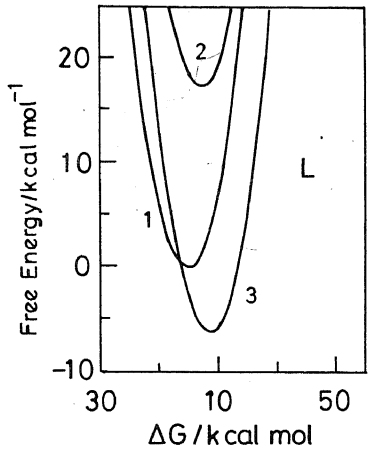


**Figure 9.** A schematic illustration of the explanation given by Chandler *et al.*[56] for the formation of $SP^+ BPL^-$ (see Figure 8). Here the state SP* is the electronic state 1, $SP^+ BCL^-$ is the electronic state 2 and $SP^+ BCL^-$ is the electronic state 3. This figure shows the calculated Marcus free energy for the diabatic surfaces for all the three states. The electron transfer occurs from 1 to 3 because it is barrierless and energetically favourable. The transfer to M branch ($1 \rightarrow 3$) involves a sizeable activation barrier.

many different time scales in biological functioning? Qualitatively, the answer to this apparently profound question is simple enough: the dynamical processes at different time scales are hierarchially coupled. An extreme example of this coupling is provided by diffusion in the supercooled liquid. Here the rapid rattling motion of a molecule in the cage formed by its neighbours is ultimately responsible for the rare jumps or hops that give rise to the diffusive mass transport. The time scales of these two motions differ by many orders of magnitude, but the slow motion would be impossible without the former. Perhaps the reason that Nature uses so many different time scales, from ultrafast to ultraslow – often separated by several orders of magnitude – is to minimize the scope of making mistakes. This is probably developed by natural selection over many years.

## Conclusion

With the advancement of ultrafast spectroscopy in the last decade, many important discoveries have been made which have helped in solving some long-standing puzzles in chemistry and biology. For example, one was puzzled by the absence of dynamic solvent effects on various charge transfer reactions in water. The paradox was partly due to the known result that the dielectric relaxation in water is about 9 ps, which is quite long. Only last year was it discovered that solvation dynamics in water is more than two orders of magnitude faster. This explains why we do not see the above-mentioned solvent dynamic effects in water. Similarly, the recent understanding of electron transfer reactions, especially the involvement of the high-frequency vibrational modes, has also emerged only in the last five years and again the impetus came from the discovery of novel aspects by using ultrafast spectroscopy. With the availability of femtosecond lasers in many laboratories around the world, we can look forward to many more such interesting discoveries in the near future.


1. Fleming, G. R. and Wolynes, P. G., *Phys. Today*, 1990, **43**, 36.
2. Bagchi, B., *Annu. Rev. Phys. Chem.*, 1989, **1989**, 115.
3. Barbara, P. F. and Jarzeba, W., *Adv. Photochem.*, 1990, **15**, 1.
4. Maroncelli, M., McInnis, J. and Fleming, G. R., *Science*, 1990, **243**, 1990.
5. Bagchi, B. and Chandra, A., *Adv. Chemys.*, 1991, **40**, 1.
6. Maroncelli, M., *J. Mol. Liq.*, 1993, **57**, 1.
7. Y. Gauduel, *J. Mol. Liq.*, 1995, **63**, 1.
8. Rossky, P. J. and Simon, J. D., *Nature*, 1994, **370**, 263.
9. Gauduel, Y. and Rossky, P. J. (eds), *Ultrafast Reaction Dynamics and Solvent Effects*, AIP Press, New York, 1994.
10. Simon, J. D. (ed.), *Ultrafast Dynamics of Chemical Systems*, Academic, Kluwer, 1994.
11. Jimnez, R., Fleming, G. R., Kumar, P. V. and Maroncelli, M., *Nature*, 1994, **369**, 471.
12. Fleming, G. R., *Chemical Applications of Ultrafast Spectroscopy*, Oxford University Press, Oxford, 1986.
13. Bagchi, B., Fleming, G. R. and Oxtoby, D. W., *Chem. Phys.*, 1986, **86**, 257.
14. Onsager, L., *Can. J. Chem.*, 1977, **55**, 1819.
15. Calef, D. F. and Wolynes, P. G., *J. Chem. Phys.*, 1983, **78**, 4145.
16. Chandra, A. and Bagchi, B., *J. Chem. Phys.*, 1989, **91**, 2594.
17. Tachiya, M., *Chem. Phys. Lett.*, 1993, **203**, 164.
18. Roy, S. and Bagchi, B., *Chem. Phys.*, 1994, **183**, 207.
19. Rosenthal, S. J., Xie, X., Du, M. and Fleming, G. R., *J. Chem. Phys.*, 1991, **95**, 4715.
20. Maroncelli, M., *J. Chem. Phys.*, 1991, **94**, 2084.
21. Neria, N. and Nitzan, A., *J. Chem. Phys.*, 1992, **96**, 5433.
22. Roy, S. and Bagchi, B., *J. Chem. Phys.*, 1993, **99**, 1310, 9938.
23. Roy, S. and Bagchi, B., *Adv. Chem. Phys.*, 1995, under preparation.
24. Nandi, N., Roy, S. and Bagchi, B., *J. Chem. Phys.*, 1995, **102**, 1390.
25. Roy, S., Komath, S. S. and Bagchi, B., *J. Chem. Phys.*, 1993, **99**, 3139.
26. Marcus, R., *Annu. Rev. Phys. Chem.*, 1964, **15**, 153.
27. Zusman, L. D., *Chem. Phys.*, 1980, **49**, 295.
28. Hynes, J. T., *J. Chem. Phys.*, 1986, **90**, 3701.
29. Weaver, M., *Chem. Rev.*, 1992, **92**, 463.
30. Barbara, P. F., *et al.*, *J. Chem. Phys.*, 1992, **96**, 3728, 7859.

31. Smith, B. B., Staib, A., Hynes, J. T., *Chem. Phys.*, 1993, **176**, 521.
32. Roy, S. and Bagchi, B., *J. Phys. Chem.*, 1994, **98**, 9207.
33. Roy, S. and Bagchi, B., *J. Chem. Phys.*, 1995, in press.
34. Miller, J. R., Calcaterra, L. T., Closs, G. L., *J. Am. Chem. Soc.*, 1984, **106**, 3047.
35. Mataga, N., Asahi, T., Kanda, Y., Okada, T. and Kakitani, T., *Chem. Phys.*, 1988, **127**, 249.
36. Asahi, T. and Mataga, N., *J. Phys. Chem.*, 1991, **95**, 1956.
37. Bixon, M. and Jortner, J., *Chem. Phys.*, 1993, **176**, 467.
38. Tominaga, K., Walker, G. C., Jarzeba, W. and Barbara, P. F., *J. Phys. Chem.*, 1991, **95**, 10475.
39. Nagasawa, Y., Yartsev, A. P., Tominaga, K., Johnson, A. E. and Yoshihara, K., *J. Am. Chem. Soc.*, 1993, **115**, 7922; Kandori, H., Kemnitz, K. and Yoshihara, K., *J. Phys. Chem.*, 1992, **96**, 8042.
40. Murata, S. and Tachiya, M., *J. Am. Chem. Soc.*, 1994, **116**, 2434.
41. Gayathri, N. and Bagchi, B., *J. Mol. Struc. (Theor. Chem.)*, 1995, in press.
42. Gayathri, N. and Bagchi, B., *J. Chem. Phys.*, submitted.
43. Bagchi, B., *Int. Rev. Phys. Chem.*, 1987, **6**, 1.
44. Kramers, H., *Physica*, 1940, **7**, 284.
45. Velsko, S. P., Waldeck, D. H. and Fleming, G. R., *J. Chem. Phys.*, 1983, **78**, 249.
46. Rothenbergere, G., Negus, D. K. and Hochstrasser, R. M., *J. Chem. Phys.*, 1983, **79**, 5360.
47. Flom, S. R., Brearley, A. M., Kahlow, M. A., Nagarajan, V. and Brabara, S. R., *J. Chem. Phys.*, 1985, **83**, 1993.
48. Nitzan, A., *Adv. Chem. Phys.*, 1988, **70**, 489.
49. Grote, R. F. and Hynes, J. T., *J. Chem. Phys.*, 1980, **73**, 2715.
50. Bagchi, B. and Oxtoby, D. W., *J. Chem. Phys.*, 1983, **78**, 2735.
51. Bagchi, B. and Fleming, G. R., *J. Phys. Chem.*, 1990, **90**, 9.
52. Sundstrom, V. and Gilbro, T., *J. Chem. Phys.*, 1984, **81**, 3463.
53. Todd, D. C. and Fleming, G. R., *J. Chem. Phys.*, 1993, **98**, 269.
54. Nokowa, L., Schwarzer, D., Troe, J. and Schreder, J., *J. Chem. Phys.*, 1992, **97**, 4827.
55. Michel-Beyerle, M. E., (ed.), *Reaction Centres of Photosynthetic Bacteria*, Springer, Berlin, 1991.
56. Chandler, D., Gehlen, J. N. and Marchi, M., in *Ultra-fast Reaction Dynamics and Solvent Effects* (eds Gauduel, Y. and Rossky, P. J.), AIP Conf. Proc., Vol. 298, 1993.
57. Dobler, J., Zinth, W., Kaiser, W. and Desterhelt, D., *Chem. Phys. Lett.*, 1988, **144**, 215.
58. Honig, B., Ebery, T., Callender, R. H., Dinur, U. and Ottolenghi, M., *Proc. Natl. Acad. Sci. USA*, 1979, **76**, 2503.
59. Austin, R. H., Beeson, K. W., Eisenstein, L., Frauenfelder, H. and Gunsalus, C., *Biochemistry*, 1975, **14**, 5355.
60. Frauenfelder, H. and Wolynes, P. G., *Science*, 1985, **229**, 337.

ACKNOWLEDGEMENTS. The work reported here was carried out in collaboration with my students. I would particularly like to thank Srabani Roy, N. Gayathri, Dr A. Chandra and Dr N. Nandi for help and discussions. I thank Prof. P. Balaram and Ms N. Gayathri for a critical reading of the manuscript. It is a pleasure to thank Prof. Paul Barbara, Prof. Graham Fleming, Prof. Mark Maroncelli, Prof. A. Nitzan, Prof. Iwao Ohmine, Prof. Masonari Tachiya and Prof. Keitaro Yoshihara for many correspondences and discussions. I also thank Dr K. Bhattacharya, Dr P. K. Das, Dr S. Umapathy, Prof. D. Mukherjee and Prof. V. Krishnan for helpful discussions. Prof. C. N. R. Rao has always been a source of encouragement during the course of the work. This work was supported, in part, by the Council of Scientific and Industrial Research, India.

Received 26 April 1995; accepted 2 May 1995

# Membrane current and potential change during neurotransmission in smooth muscle

**Rohit Manchanda**

School of Biomedical Engineering, Indian Institute of Technology, Powai, Bombay 400 076, India

**Smooth muscle cells are electrically coupled to one another in a syncytium, and this renders their electrophysiology during neurotransmission strikingly different from that at other synapses. The postjunctional depolarizing responses of sympathetically innervated smooth muscle such as the vas deferens, particularly, the excitatory junction potentials (EJPs), possess intriguing properties which for several years have resisted explanation. A principal issue has been the temporal relationship of transmitter-generated membrane current to the resulting potential change, which seems to differ depending upon whether transmitter release is spontaneous or is nerve-stimulation-evoked. Accordingly, smooth muscle electrical properties appear to change with different patterns of transmitter release. Until some years ago this relationship was an area of uncertainty, firstly because transmitter-activated membrane current could not be measured directly and secondly because intracellular membrane potential measurements gave rise to conflicting results. Many of the uncertainties have now been resolved with refinements in techniques of measurement that have allowed membrane current time course during neurotransmission to be estimated. As a result, our understanding of smooth muscle electrical properties has been clarified and deepened. These developments are outlined in this review, and it is shown how our comprehension of neurotransmission has at every stage been influenced strongly by the techniques adopted for investigation.**